Silicon (2017) 9:711–715
DOI 10.1007/s12633-016-9429-5

ORIGINAL PAPER

Design and Fabrication of Protection Window Against YAG Laser

Y. H. Elbashar[1]

Received: 3 July 2015 / Accepted: 6 March 2016 / Published online: 31 May 2016

Abstract Window protection glass against a YAG laser based on a bandpass absorption filter was fabricated from bismuth oxide doped copper phosphate glass with series of xBi_2O_3-(40-x) ZnO-10Na_2O-6Cu_2O-44P_2O_5 in molar ratio with x=0, 5 and 10 and were prepared by using a conventional glass casting and quenching technique. The density was measured by the conventional Archimedes method and the molar volume was calculated. Bismuth oxide is a heavy element; by increasing the doping in a glass composition it can cause an unusual phenomenon between the density and molar volume, they can have the same trend. The glass was investigated by using the XRD technique, which proved the systems are completely in the glass state. Optical spectroscopic analysis of the glass filter from the transmittance data showed the UV and the IR cut-off bands to the bandpass filter, which confirmed the band absorption in the IR cut-off included the Nd:YAG laser wavelength, which can be used for a glass laser safety window.

Keywords Laser safety · Absorption filter · YAG laser window protection · Bandpass filte

Highlights

- xBi_2O_3- (40-x) ZnO-10Na_2O- 6Cu_2O-44P_2O_5 in molar ratio with x=0, 5, and 10
- The density and molar volume followed the abnormal behavior.
- The UV bandstop covered the range from 190 nm to 451 nm
- The IR bandstop covered the range from 638 nm to 1250 nm which covers the YAG laser wavelength
- The glass is low cost and can be used as a protection glass window against a YAG laser

1 Introduction

Nowadays, the increase of glass researches is due to their applications in photonics and nuclear areas [1–7]. The idea of protective materials from nuclear radiation finds increasing interest due to the expansion of the use of nuclear technology. This technology depends on optical materials like glass, and it must be transparent in the visible light and absorbed or reflected in the unused wavelength band. Copper doped phosphate has double band absorptions, one in the UV band and the other in the IR band [8–11]. To increase the the IR absorption band we should add some transition metals like Bi_2O_3, and to decrease the hygroscopic effect of the phosphate glass we should add other transition metals like ZnO[12–14].

A YAG laser with a wavelength of 1064 nm is used in many applications like material processing, medicine, spectroscopy, and metrology, etc. The development of a window against this type of wavelength is very important, due to the rapid development of the technology of this type of laser system [15–18]. Humans need two types of protection against the high power Nd:YAG lasers, the room window, and the eye goggles. The room window is replaceable due to it being very near the laser light source, light scattering, gas plume, sparks, or any other heating sources that can be

✉ Y. H. Elbashar
y_elbashar@yahoo.com

[1] Department of Physics, Faculty of Science, Aswan University, Aswan, Egypt

very hazardous to the user of the device. The YAG window must have a good transmission wavelength in the visible spectrum, and an excellent protection against the specific wavelength. Also, we need to decrease the light transmission during the laser material processing in the laser room to protect the human eye, skin, and any other related organisms. The laser protection window must be very cheap, and have a long lifetime. The laser protection window in this paper will depend on the absorption phenomenon, rather than reflection. The manufacturing of this glass will be applicable and producible by to the optical glass industry, unlike other techniques used before in YAG laser protection. The copper doped phosphate glass is excellent for this type of application, the changing of doping can increase to the near infrared absorption band, which can cover the YAG laser band at 1064 nm and some other lasers wavelengths [19–45]. The aim of this work is to design and fabricate a protection glass window against laser scattering in the field of laser working. This study is unique for this type of glass and its application in YAG laser window protection.

2 Experimental

The glass samples consisting of copper oxide doped phosphate glass with a chemical composition xBi_2O_3-(40-x) ZnO-10Na_2O-6Cu_2O-44P_2O_5 in molar ratio with x=0, 5, and 10 were prepared by the conventional melt and quenching technique. The starting materials used were $NaCO_3$, ZnO, $(NH_4)H_2PO_4$, Bi_2O_3, and Cu_2O. The chemical compositions were mixed and ground using a mortar for 30 min for each sample, and then calcinated in a porcelain crucible using a muffle furnace for 1hour at 290 ^oC to remove the gases from the chemicals like CO_2 and NH_3. After that the sample was moved to a melting furnace for 30 min at 1100 ^oC, then shaking clockwise to ensure the material had high homogeneity. Finally, the casting was quenched and annealed in a copper mold 290 °C with a pressing plate to form a thin disk for studying the optical properties.

The annealing technique is required because of the internal stress that remained in the glass during the quenching. The samples were investigated by a polarizer technique before optical that density measurement and found all samples are free from the thermal stresses. Optical microscopy was used to investigate the samples for the porosity, and and some was found to occur during the pouring of the molten glass. In this study some measurements to were made characterize the glass samples, including density, XRD, absorbance, and transmission. The density was measured by the simple Archimedes method for all the glass samples using ethanol as an immersion liquid at room temperature, the measurements of the samples were repeated three times with accuracy ±0.01. Molar volume was calculated from the density. The X-ray powder diffraction (XRD) curves for the prepared glasses samples were obtained using a Bruker AXS D8 Advance XRD diffractometer. The optical transmittance was recorded at room temperature, UV/Vis/IR transmission spectra obtained for the disk glass samples with the two parallel polished faces were measured using a (JASCO – V570) spectrophotometer in the wavelength range 190 - 1300 nm.

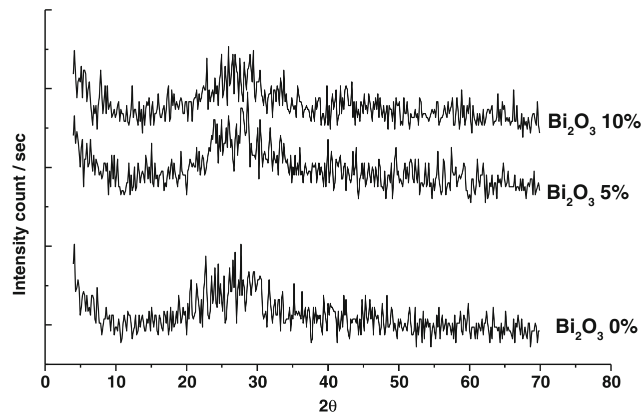

Fig. 1 XRD curves for the prepared glass

3 Results and Discussion

The XRD measurement for the glass powder found no crystal growth in the glass samples, and the annealing temperature did not result in any crystal growth in the samples. As shown in Fig. 1 the material is completely amorphous, with no sharp peaks in the XRD curves.

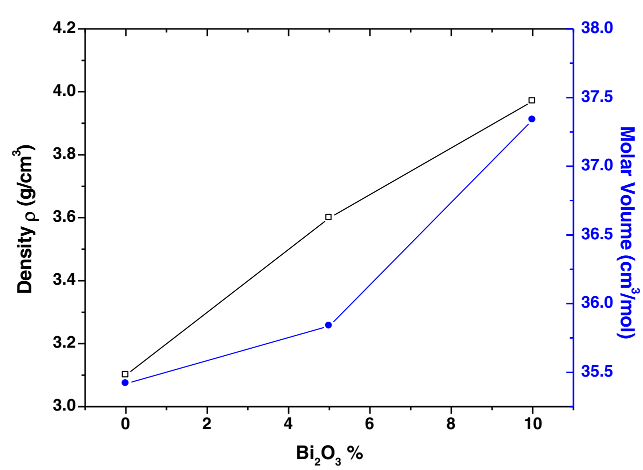

Fig. 2 Density and Molar volume as a function of Bi_2O_3 contents

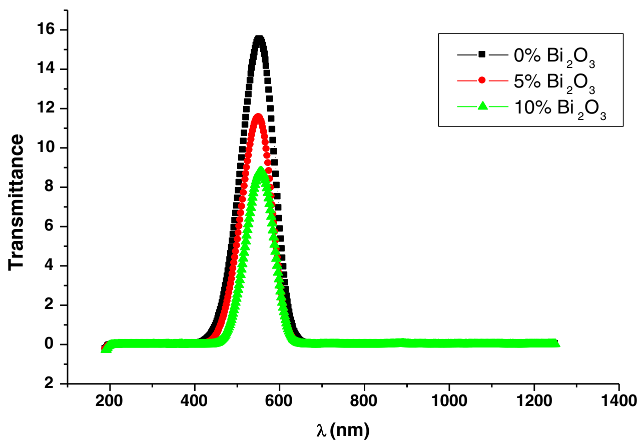

Fig. 3 Transmission verses wavelength of the glass samples

The density and molar volume V_M were calculated according to the relations [1]:

$$\rho = \left[\frac{W_{air}}{(W_{air} - W_l)}\right]\rho_0 \quad (1)$$

$$V_M = \frac{M_{W(glass)}}{\rho_{glass}} \quad (2)$$

Where ρ the is sample density, ρ_0 the liquid density, W_{air} the weight in the air, W_l the weight in the liquid, V_M the molar volume and M_w the molar mass.

The density of the glass samples increases with increasing to Bi content as shown in Fig. 2. The normal trend of the density and molar volume is opposite to each other, but in some cases the trend of the density and molar volume is the same. The reason for this trend in our glass composition is because the molar mass of bismuth oxide is heavier than the molar mass of zinc oxide. So, the glass network matrix with higher contents of bismuth oxide Bi^+ has higher density.

Table 1 The variation of UV and IR cut-off with the bismuth oxide content

	Bi_2O_3 0 %	Bi_2O_3 5 %	Bi_2O_3 10 %
UV Cut-off (nm)	417	431	451
UV bandstop	190-417	190-431	190-451
IR Cut-off (nm)	638	649	664
IR bandstop	638- 1250	649- 1250	664- 1250

In addition, the increase of molar volume is due to the atomic radius of Bi^+ being higher than Zn^+. Since, Bi_2O_3 has a high relative molecular mass this opens the structure of the glass network and introduces excess structure volume due to the number of oxygen atoms that are connected to the bismuth oxide. ZnO acts as a modifier, and the replacement of ZnO by Bi_2O_3 causes increases of overall molar volume.

The variation of optical transmission of the glass samples shown in Fig. 3 is due to the strong absorption coefficient of copper in the UV and IR, but the transmission of the light decreases due to the bismuth oxide content. Otherwise, the bismuth oxide gives a good absorption in the near infrared band that reaches to 1250 nm which is covers the YAG laser band. Moreover, all the bandpass filters produced in this study can be used as a YAG laser window protection, but with a variation in the transmission when used in different applications.

The UV cut-off and UV bandstop filter are shown in Fig. 4. The bandstop in optics is a technique that is able to reject a band of spectral lines. For this filter the UV bandstop begins with 190 nm and increases with increasing the Bi_2O_3 doping. The increase of bismuth oxide gives a good decrease to the transmission, but it also affects the bandstop as shown in Table 1. The UV cut-off is the end of the band-

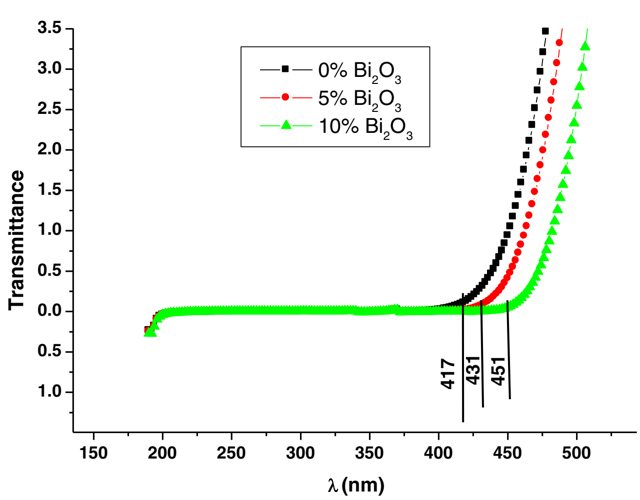

Fig. 4 UV cut-off verses wavelength of the glass samples

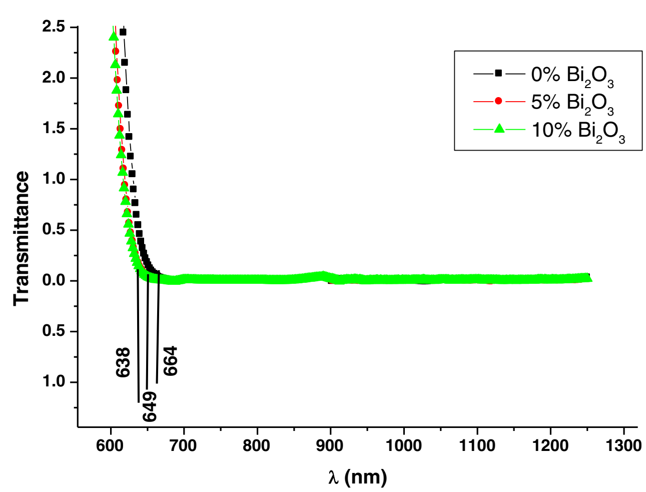

Fig. 5 IR cut-off verses wavelength of the glass samples

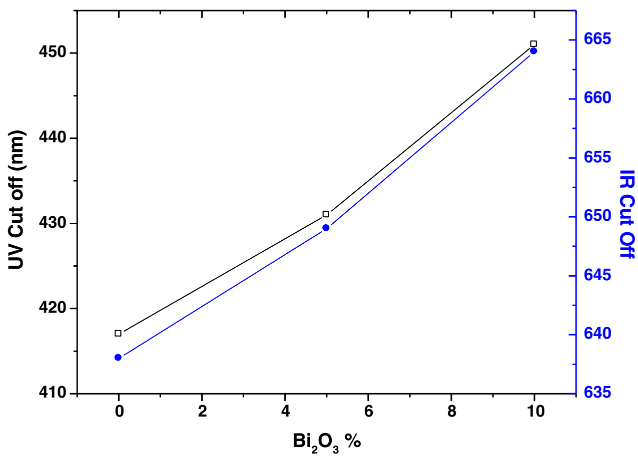

Fig. 6 UV and IR cut-off as a function of Bi_2O_3 contents

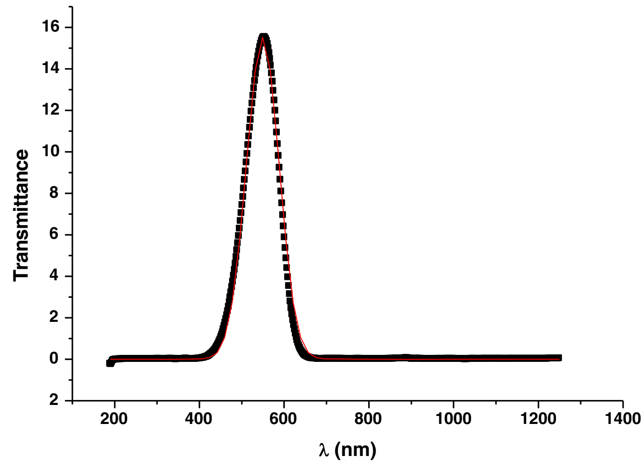

Fig. 7 The integration of the transmission peak

stop filter which starts from 417nm to 451nm depending on the bismuth oxide concentration from % to 10 % and with a constant 6 % Cu_2O concentration.

The IR cut-off and IR bandstop filter are shown in Fig. 5. The bandstop in the IR band is different than the UV cut-off and UV bandstop. For this filter the IR bandstop begins with 634 nm, 664 nm, and ends at 1250 nm which is the end of the measurement of the transmission. Table 1 shows the UV, IR cut-off, and bandstop for both. It is found that the variation between the bismuth oxide content, UV cut-off, and IR cut-off are linear increasing as shown in Fig. 6.

The bandpass in optics is a technique that is able to pass a band of spectral lines, in this study it is in the visible region. These filters have a single bandpass with a double band-stop in the UV and IR as shown. The area and the center of the bandpass are calculated as shown in Table 2. This technique is very cheap for use as a in laser protection window, and the final finishing needs no extra effort in the product. The center of the peaks as shown in Fig. 7 shows these filters in the green band, nearly attached to the blue band The bandstop in the infrared covers the region that is used in some laser protection windows like semiconductor lasers that operate at 808 nm and Nd:YAG or Nd:Glass that operate from 1050 nm to 1060 nm , which can be used as a laser protection window with any wavelength cover from 638 nm to 1250nm.

Table 2 The area, center, and the peak width of the bandpass filter

	Bi_2O_3 0 %	Bi_2O_3 10 %	$Bi_2O_3$15 %
Area	1502.3	1037.8	721
Center (nm)	549.3	547.2	553
Width (nm)	77.28	71.5	65.1

4 Conclusion

The present study shows the effect on Bi_2O_3 of the phosphate glass a constant Cu_2O with 6 % content. The molar volume and density are studied to describe the effect of the bismuth oxide on the phosphate glass and the unusual trend between the density and molar volume. The optical transmission is also studied and presents the effect of Bi ions on the cut-off for the UV and infrared bands. The practicality of using this type of glass as bandpass filters is indicated by all glass samples showing a bandstop in the UV bandstop and infrared bands , which is an excellent protection window for laser safety against a YAG laser.

References

1. Saeed A, El shazly RM, Elbashar YH, Abou El-azm AM, El-Okr MM, Comsan MNH, Osman AM, Abdal-monem AM, El-Sersy AR (2014) Gamma ray attenuation in developed borate glassy system. Radiat Phys Chem 102:167–170
2. Rayan DA, Elbashar YH, El Basaty AB, Rashad MM (2015) Infrared spectroscopy of cupric oxide doped barium phosphate glass. Research Journal of Pharmaceutical, Biological and Chemical Sciences (RJPBCS) 6(3):1026–1030
3. Elhaes H, Attallah M, Elbashar Y, Ibrahim M, El-Okr M (2014) Application of Cu2O-doped phosphate glasses for bandpass filter. J Phys B Condensed Matter 449(15):251–254
4. Aboulfotoh N, Elbashar Y, Ibrahem M, Elokr M (2014) Characterization of copper doped phosphate glasses for optical applications. J Ceramics Int Part B 40(7):10395–10399
5. Elhaes H, Attallah M, Elbashar Y, Al-Alousi A, El-Okr M, Ibrahim M (2014) Modeling and optical properties of P2O5-ZnO-CaO-Na2O glasses doped with copper oxide. J Comput Theor Nanosci 11(10):2079–2084
6. Rayan DA, Elbashar YH, Rashad MM, El-Korashy A (2013) Spectroscopic analysis of phosphate barium glass doped cupric oxide for bandpass absorption filter. J Non-Cryst Solids 382(15):52–56

7. Sutter E, Schirmacher A (2001) Protective area of laser eye protectors. Opt Laser Technol 33:255–8
8. Elbashar YH, Saeed A (2015) Computational spectroscopic analysis by using Clausius–Mossotti method for sodium borate glass doped neodymium oxide. Research Journal of Pharmaceutical, Biological and Chemical Sciences (RJPBCS) 6(5):320–326
9. Saeed A, Elbashar YH, El Kameesy SU (2015) Study of Gamma Ray Attenuation of High-Density Bismuth Silicate Glass for shielding applications. Research Journal of Pharmaceutical, Biological and Chemical Sciences (RJPBCS) 6(4):1830–1837
10. Saeed A, Elbashar YH, El Kameesy SU (2015) Towards modeling of copper-phosphate glass for optical bandpass absorption filter. Research Journal of Pharmaceutical, Biological and Chemical Sciences (RJPBCS) 6(4):1390–1397
11. Yahia HE (2015) Structural and spectroscopic analyses of copper doped P2O5-ZnO- K2O-Bi2O3 glasses. Int J Process Appl Ceram 9(3):169–173
12. ElBatal FH, Marzouk MA, Abdelghany AM (2010) UV–visible and infrared absorption spectra of gamma irradiated V 2 O 5-doped in sodium phosphate, lead phosphate, zinc phosphate glasses: A comparative study. J Non-Cryst Solids 357(3):1027–1036
13. ElBatal HA, Abdelghany AM, ElBatal FH, ElBadry KM, Moustaffa FA (2011) UV–visible and infrared absorption spectra of gamma irradiated CuO-doped lithium phosphate, lead phosphate and zinc phosphate glasses: a comparative study. Phys B Condens Matter 406(19):3694–3703
14. Abdelghany AM, ElBatal HA (2014) Gamma-rays interactions on optical, FTIR absorption and ESR spectra of 3d transition metals-doped sodium silicophosphate glasses. J Mol Struct 1067:138–146
15. Sabatini R, Richardson MA (2003) A new approach to eye-safety analysis for airborne laser systems flight test and training operations. Opt Laser Technol 35:191–8
16. Chen M, Li C, Mai X, Wang W, Ma S, Xia Yuxue (2007) Eye-protection glasses against YAG laser injury based on the band gap reflection of one-dimensional photonic crystal. Opt Laser Technol 39(1):214–218
17. Schirmacher A., Sutter E (2001) Induced transmittance in alexandrite laser eye-protectors—a survey of different types of laser filters. Opt Laser Technol 33(5):359–362
18. Shelby JE (2005) Introduction to glass science and technology, 2nd edn. the Royal Society of Chemistry
19. Doremus RH (1994) Glass science, 2nd Ed. John Wiley & Sons Inc.
20. Brow RK (2000) Review: the structure of simple phosphate glasses. J Non-Cryst Solids 263–264(1):1–28
21. Laudisio M, Catauro EG (1999) The non-isothermal devitrification of glasses in the SrO4GeO2-BaO(4)GeO(2 c)omposition range. J Therm Ana 58(3):617–623
22. Ghoneim NA, Abdelghany AM, Abo-Naf SM, Moustafa FA, ElBadry KM (2013) Spectroscopic studies of lithium phosphate, lead phosphate and zinc phosphate glasses containing TiO 2: Effect of gamma irradiation. J Mol Struct 1035:209–217
23. Metwalli E (2003) Copper redox behavior, structure and properties of copper lead borate glasses. J Non-Cryst Solids 317:221–230
24. Barczynski RJ, Gazda M, Murawski L (2003) Mixed ionic–polaron transport and rapid crystallization in (Bi,Pb)–Sr–Ca–Cu–O glass. Solid State Ionics 157:299–303
25. Metwalli E, Karabulut M, Sidebottom DL, Morsi MM, Brow RK (2004) Properties and structure of copper ultraphosphate glasses. J Non-Cryst Solids 344:128–134
26. Miura T, Benino Y, Sato R, Komatsu T (2003) Universal hardness and elastic recovery in Vickers nanoindentation of copper phosphate and silicate glasses. J Eur Ceram Soc 23:409–416
27. Bruni S, Cariati F, Narducci D (1994) Infrared specular reflection spectra of copper-zinc phosphate glasses. Vib Spectrosc 7:169–173
28. Vedeanu N, Cozar O, Ardelean I, Lendl B (2006) IR and Raman investigation of x(CuO·V2O5)(1-x)[P2O5·CaF2] glass system. J Optoelectron Adv Mater 8:78–81
29. Vedeanu N, Magdas DA, Stefan R (2012) Structural modifications induced by addition of copper oxide to lead–phosphate glasses. J Non-Cryst Solids 358:3170–3174
30. Koo J, Bae B, Na H (1997) Raman spectroscopy of copper phosphate glasses. J Non-Cryst Solids 212:173–179
31. Walter G, Vogel J, Hoppe U, Hartmann P (2003) Structural study of magnesium polyphosphate glasses. J Non-Cryst Solids 320:210–222
32. Tischendorf B, Otaigbe JU, Wiench JW, Pruski M, Sales BC (2001) A study of short and intermediate range order in zinc phosphate glasses. J Non-Cryst Solids 282:147–158
33. Nocun M (2004) Structural studies of phosphate glasses with high ionic conductivity. J Non-Cryst Solids 333:90–94
34. Sułowska J, Wacławska I, Olejniczak Z (2013) Structural studies of copper-containing multicomponent glasses from the SiO2-P2O5-K2O-CaO-MgO system. J Vib Spectrosc 65:44–49
35. Leenakul W, Kantha P, Pisitpipathsin N, Rujijanagul G, Eitssayeam S, Pengpat K (2013) Structural and magnetic properties of SiO2–CaO–Na2O–P2O5 containing BaO–Fe2O3 glass–ceramics. J Magn Magn Mater 325:102–106
36. Asghar MH, Shoaib M, Placido F, Naseem S (2009) Modeling and preparation of practical optical filters. Current Appl Phys 9:1046–1053
37. Bessell M (2001) Encyclopedia of astronomy and astrophysics. Nature Publishing Group and Institute of Physics Publishing, UK
38. Oo HM, Kamari HM, Wan-Yusoff WMD (2012) Optical properties of bismuth tellurite based glass. Int J Mol Sci 13:4623–4631
39. Kaewjaeng S, Kaewkhao J, Limsuwan P, Maghanemi U (2012) Effect of BaO on optical, physical and radiation shielding properties of SiO2-B2O3-Al2O3-CaO-Na2O glasses system. Procedia Engineering 32:1080–1086
40. Limkitjaroenporn P (2011) Physical, optical, structural and gamma-ray shielding properties of lead sodium borate glasses. J Phys Chem Solids 72:245–251
41. Dutta A, Ghosh A (2007) Structural and optical properties of lithium barium bismuthate glasses. J Non-Cryst Solids 353(13–15):1333–1336
42. Punia R, Kundu RS, Hooda J, Dhankhar S, Dahiya S (2011) Effect of Bi2O3 on structural, optical, and other physical properties of semiconducting zinc vanadate glasses. J Appl Phys 110: 033527
43. Bae B-S, Weinberg MC (1994) Optical absorption of copper phosphate glasses in the visible spectrumOriginal research article. J Non-Cryst Solids 168(3):223–231
44. Takebe H, Nishimoto S, Kuwabara M (2007) Thermal and optical properties of CuO–BaO–B2O3–P2O5 glasses. J Non-Cryst Solids 353(13–15):1354–1357
45. Nadeem MY, Waqas AHMED (2000) Optical properties of ZnS thin films. Turk J Phys 24:651–659